Relation between microstructure and Charpy impact properties of an elemental and pre-alloyed 14Cr ODS ferritic steel powder after hot isostatic pressing

Z. Oksiuta · E. Boehm-Courjault · N. Baluc

Abstract This article describes the microstructure and Charpy impact properties of an Fe–14Cr–2W–0.3Ti–0.3Y_2O_3 oxide dispersion strengthened (ODS)-reduced activation ferritic (RAF) steel, manufactured either from elemental powders or from an Fe–14Cr–2W–0.3Ti pre-alloyed powder. ODS RAF steels have been produced by mechanical alloying of powders with 0.3 wt% Y_2O_3 nanoparticles in either a planetary ball mill or an attritor ball mill, for 45 and 20 h, respectively, followed by hot isostatic pressing (HIPping) at 1,150 °C under a pressure of 200 MPa for 4 h and heat treatment at 850 °C for 1 h. It was found that the elemental ODS steel powder contains smaller particles with a higher specific surface area and a two times higher oxygen amount than the pre-alloyed ODS steel powder. After HIPping both materials exhibit a density higher than 99%. However, the pre-alloyed ODS steel exhibits a slightly better density than the elemental ODS steel, due to the reduced oxygen content in the former material. Charpy impact experiment revealed that the pre-alloyed ODS steel has a much larger ductile-to-brittle transition temperature (DBTT) (about 140 °C) than the elemental ODS steel (about 25 °C). However, no significant difference in the upper shelf energy (about 3.0 J) was measured. TEM and SEM–EBSD analyses revealed that the microstructure of the elemental ODS steel is composed of smaller grains with a larger fraction of high-angle grains (>15°) and a lower dislocation density than the pre-alloyed ODS steel, which explains the lower DBTT value obtained for the elemental ODS steel.

Introduction

The hot isostatic pressing (HIPping) technique is a well-proven consolidation method for producing fully dense, near net shape materials. This method is also frequently used for closing the residual porosity in bulk materials, after casting for instance. The properties of materials produced by mechanical alloying (MA) and HIPping are generally similar to those obtained with conventional casting methods [1, 2]. However, the features and conditions of MA and HIPping processes have a significant impact on the mechanical strength of the obtained materials. It is well known that the mechanical properties of such materials, especially their fracture behaviour, strongly depend on the initial powder particle size morphology and on the content in impurities (e.g. O, N and C) [3]. The most suitable powder used for HIPping is an argon-gas atomized powder containing as little oxygen as possible. Indeed, the oxide layer on the surface of the powder particles strongly reduces interaction of the particles during HIPping, which may cause porosity that significantly decreases the impact fracture properties, especially the upper shelf energy (USE), of compacted materials [3–5]. The pores reduce the effective cross section of specimens and act as internal

Z. Oksiuta (✉)
Faculty of Mechanical Engineering, Bialystok Technical University, Wiejska 45c, 15-351 Bialystok, Poland
e-mail: oksiuta@pb.edu.pl

E. Boehm-Courjault
Computational Materials Laboratory, Ecole Polytechnique Fédérale de Lausanne (EPFL), STI-IMX-LSMX, Station 12, 1015 Lausanne, Switzerland

N. Baluc
Ecole Polytechnique Fédérale de Lausanne (EPFL), Centre de Recherches en Physique des Plasmas, Association Euratom-Confédération Suisse, 5232 Villigen PSI, Switzerland

notches initiating cleavage fracture. It was reported in the literature that the HIPped materials produced using a mechanically alloyed, gas atomized powder exhibit a relatively low impact fracture performance [5–7], due to a relatively high impurity content and work hardening amount, which increase the porosity level as well as the hardness and tensile strength of materials and decrease their impact fracture resistance. Therefore, the mechanical performance of as-HIPped specimens, such as tensile behaviour and fracture toughness, strongly depend on the initial powder size and morphology, the porosity and shape of pores remaining after consolidation as well as the impurities content. Recently, HIPping process has been also used for the production of oxide dispersion strengthened (ODS) ferritic steels as an alternative consolidation method to hot pressing or hot extrusion (HE) for obtaining a more homogeneous, isotropic and fine-grained microstructure.

ODS-reduced activation ferritic (RAF) steels are attractive materials for advanced nuclear installations due to their excellent high temperature mechanical strength, high resistance to neutron irradiation-induced swelling and good corrosion resistance due to high chromium and low carbon contents [8–10]. The ODS RAF steels are usually manufactured by powder metallurgy. The use of the powder metallurgy technique for producing ODS RAF steels yields the formation of bulk materials with a high density of nanoclusters enriched with Y, Ti and O, which significantly reinforce the steels at high temperatures (increasing their creep resistance) and also allow a strong improvement in their radiation resistance. However, there are still some problems with the manufacturing route of ODS RAF steels. The main issue arising during manufacturing, especially during MA, is the increase in impurities contents in the steels, which have a detrimental influence on their density and mechanical properties. Our preliminary results revealed that it is difficult to obtain a fully dense ODS RAF steel from elemental Fe, Cr, W and Ti powders, despite varying the HIPping parameters [11]. As a consequence, fracture properties of such steels are still far away from acceptance.

In this work, ODS RAF steels with the nominal composition of Fe–14Cr–2W–0.3Ti–0.3Y_2O_3 (wt%) have been produced by MA and HIPping, either from elemental powders or using a Fe–14Cr–2W–0.3Ti pre-alloyed powder. The relative density, microstructure and Charpy impact properties of as-compacted ingots of both types of material have been analysed. The main goal of this work was to find out a correlation between the microstructure and the Charpy impact properties of the as-HIPped steels by using in particular electron back-scattered diffraction (EBSD) analysis to determine the grain misorientation in the materials.

Experimental procedure

Two types of Fe–14Cr–2W–0.3Ti–0.3Y_2O_3 ODS RAF steel powders were prepared by: (i) MA of elemental Fe, Cr, W and Ti powders with 0.3Y_2O_3 nanoparticles in a planetary ball mill, in a hydrogen atmosphere, for 45 h, which is referred to hereafter as the elemental ODS powder, or (ii) MA of a pre-alloyed, argon-gas atomized Fe–14Cr–2W–0.3Ti steel powder (Aubert&Duval Co, France) with 0.3Y_2O_3 nanoparticles in an attritor ball mill (Plansee, Austria), in a hydrogen atmosphere, for 20 h, which is referred to hereafter as the pre-alloyed ODS powder. About 10 kg of pre-alloyed ODS steel powder could be produced in a single batch, while only about 0.1 kg of elemental ODS steel powder could be produced at once. Therefore, several milling experiments had to be performed to obtain 1 kg of elemental ODS steel powder. After MA both ODS steel powders were HIPped at 1,150 °C under a pressure of 200 MPa for 4 h, followed by annealing at 850 °C for 1 h in vacuum and cooling down slowly to ambient temperature.

Powders and ingots were examined by (i) scanning electron microscopy (SEM) in a Zeiss NVision 40, (ii) transmission electron microscopy (TEM) in a JEOL 2010 and (iii) EBSD using a XL30FEG SEM (Philips Electronics Instruments Corp., USA) equipped with a Nordlys II CCD camera and with the 'Channel 5' acquisition system (Oxford-HKL, UK). An accelerating voltage of 20 kV, a spot size of 4 (few nanometres) and a working distance of about 13 mm were used as measurement parameters. For grain identification, a disorientation criterion of 5° was used.

For EBSD analyses, surface preparation of the specimens is critical. ODS steels were first ground with increasingly fine SiC papers lubricated with water (grade 1000–4000) and then polished to mirror quality using 1- and 0.25-μm diamond sprays and DP-Nap clothes (Struers, Denmark) lubricated with ethanol. In order to remove the mechanically deformed thin surface layer, a final polishing step was necessary: it was done on a OP-Chem cloth (Struers) with a 10 vol% H_2O_2–OP-S silica suspension (Struers).

Microhardness measurements were carried out using a Vickers diamond pyramid (JENOPHOT 2000) by applying a load of 0.98 N for 15 s. An average particle size of the powders was measured upon the SEM images by means of computer image analysis. The specific surface area of the powders after MA was measured by means of the BET method. Chemical analyses of the powders were performed using wavelength dispersive X-ray fluorescence spectroscopy (WD-XRF) as well as LECO TC-436 and LECO IR-412 analysers for measurements of O, N and C contents, respectively. The relative density of the ODS ingots was

measured by means of the Archimedes method using an analytical balance KERN ARJ 220-4M.

Charpy impact tests were performed on KLST specimens ($3 \times 4 \times 27$ mm^3) between -100 and 300 °C, using an instrumented Charpy impact machine with an energy capacity of 30 J. The ductile-to-brittle transition temperature (DBTT) was determined by means of a sigmoidal fit based on the Boltzmann equation $y = (USE - LSE)/2 + LSE$, where USE is the upper shelf energy and LSE is the lower shelf energy.

Results

Characterization of the powders

The chemical composition of the ODS steel powders after MA is shown in Table 1. The elemental ODS powder contains a high oxygen amount although the milling process was carried out in a pure hydrogen atmosphere. As expected, the elemental ODS steel powder contains more than two times higher oxygen amount than the pre-alloyed one. This is not only due to a longer milling time of elemental powders in comparison to the pre-alloyed one, but also due to the fact that before milling the elemental

Table 1 Chemical composition of the ODS steel powders after mechanical alloying in hydrogen (in wt%)

Elements	Elemental ODS powder	Pre-alloyed ODS powder
C	0.067	0.043
Mn	0.02	0.38
Cr	13.8	13.5
W	2.21	1.92
Ti	0.32	0.33
Y	0.28	0.26
O	0.372	0.172
N	0.053	0.005
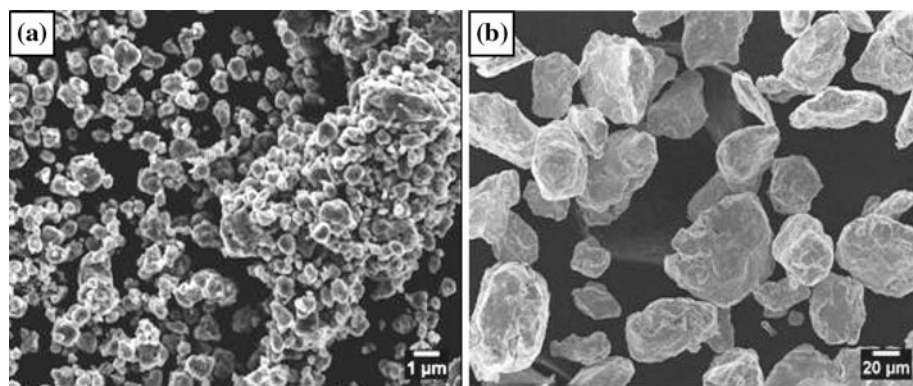
Table 2 Features of the ODS steel powders

ODS powder	BET (m^2/g)	$\mu HV_{0.1}$	Particle size (μm)
Pre-alloyed, mechanically alloyed in an attritor	0.0663 ± 0.0003	744.9 ± 30.6	44.8 ± 12.4
Elemental, mechanically alloyed in a ball mill	0.1272 ± 0.0001	825.2 ± 65.9	12.3 ± 6.1

powders were already containing a total amount of about 0.3 wt% of oxygen, whereas the pre-alloyed powder was containing only about 0.09 wt% of oxygen.

The morphology of both types of powder after MA is shown in Fig. 1. The elemental ODS powder contains more than three times smaller particles and exhibits a larger specific surface area, by about 50%, than the pre-alloyed one (see Table 2). The microhardness of the powders after MA is relatively high and similar for both types of powder, as it is emphasized in Table 2. However, about 10% higher microhardness values were measured in the case of the elemental ODS powder. This is due to the higher impact energy provided by the planetary ball mill, which results in a higher degree of work hardening, as compared to the attritor device.

As it can be seen in Fig. 2, both types of powders have a strongly deformed, complex, nano-sized microstructure. TEM images show that both powders contain nano-grains, elongated in the direction parallel to the surface of the particles, from 40 nm in thickness up to 120 nm in length.

Microstructure of HIPped ingots

In general, a residual porosity was observed in both types of ODS RAF steel after HIPping. The density of the pre-alloyed ODS steel, equal to 7.80 g/cm^3, was found slightly higher than the one of the elemental ODS steel, equal to 7.78 g/cm^3, probably due to lower amount of oxygen

Fig. 1 SEM images of the **a** elemental and **b** pre-alloyed ODS steel powders after mechanical alloying

**Fig. 2** TEM images of the **a** elemental and **b** pre-alloyed ODS steel powders after mechanical alloying
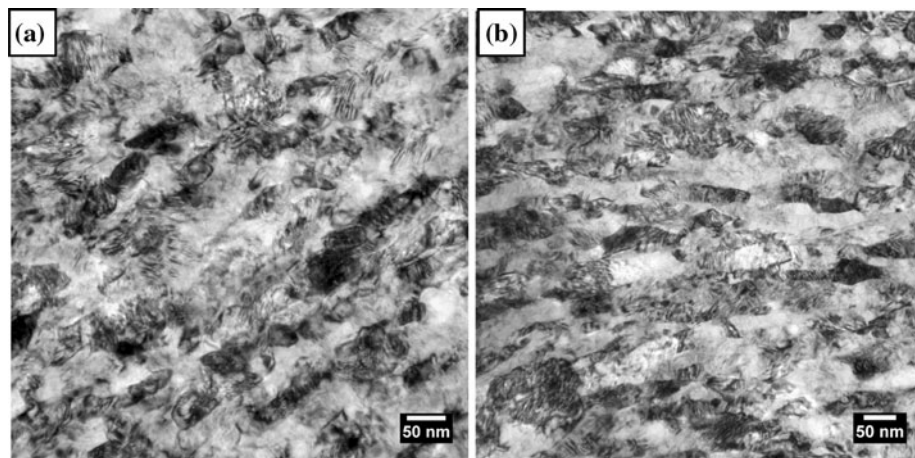

contained in the former material. The theoretical density of the ODS steel was calculated and found equal to 7.83 g/cm^3. Isolated pores (with a size up to 1 μm) were observed by optical microscopy in the case of both materials.

Typical TEM images of both types of ODS steels after consolidation are shown in Fig. 3. Both materials are composed of a ferritic (bcc) matrix that contains equiaxed grains and about few hundreds nanometres in size oxide impurities. In the case of the elemental ODS steel these impurities are mostly Ti and Cr oxides, while in the case of the pre-alloyed ODS steel Ti and Al oxide particles were found using an EDX detector. These impurities are usually located at the prior particle boundaries and some of them at the grain boundaries as it is shown in Fig. 3c. It is noteworthy that smaller oxide particles were observed in the case of the pre-alloyed ODS steel. This can be related to

Fig. 3 TEM images of the ODS steels after HIPping, manufactured from **a** an elemental powder, **b** a pre-alloyed powder, general view, **c** a pre-alloyed powder, oxide particles, **d** dark field images of the nanoparticles of the pre-alloyed ODS steels
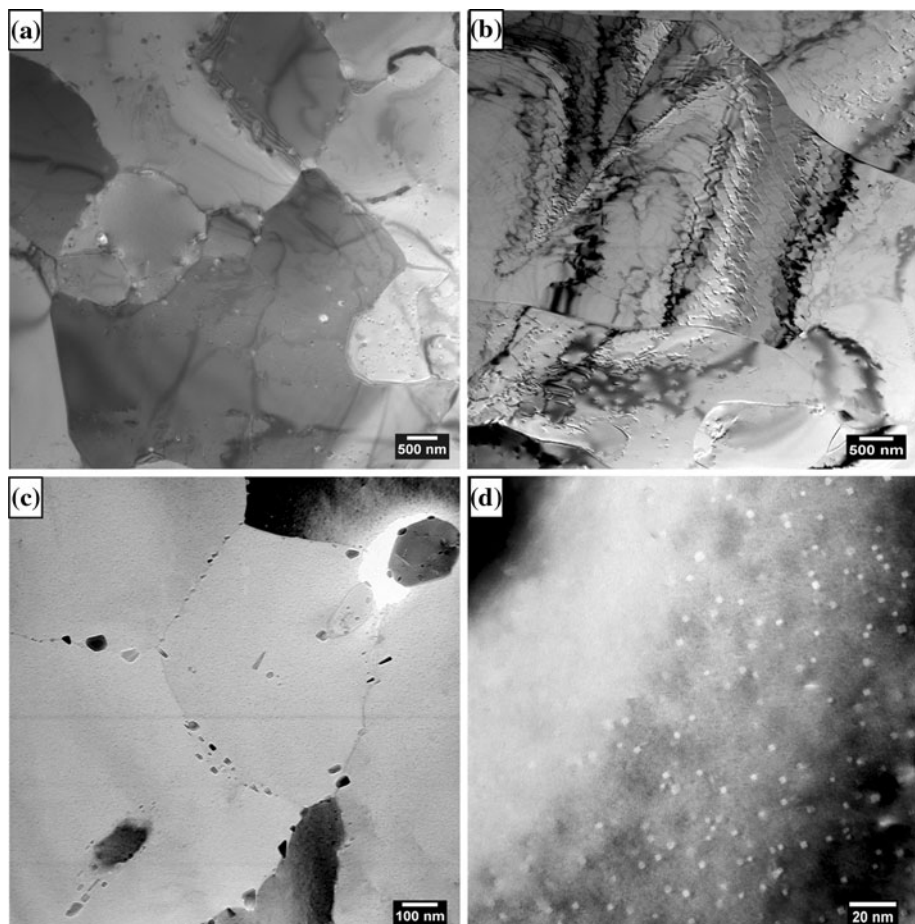
the lower oxygen content measured for this material. Significant differences in the grain size and dislocation density were observed. The pre-alloyed ODS steel (Fig. 3b, c) exhibits a rather complex microstructure that consists of prior particle boundaries, with a shape and size similar to those of the pre-alloyed powder, and equiaxed grains, located inside the prior particles and having a size up to 20 μm, and a higher dislocation density in comparison to the elemental ODS steel (Fig. 3a).

More particular TEM observations of the pre-alloyed ODS steel revealed areas with arrays and tangles of dislocation as well as dislocation free areas. A number of the coarse grains appear composed of smaller grains with a size of a few microns. Finer and more homogeneous grains, with an average size of about 2 μm and a lower dislocation density, were observed in the case of the elemental ODS steel (Fig. 3a). SEM observations of the microstructure also confirmed that the ODS RAF steel produced from

elemental powders is composed of smaller grains. Both alloys also contain very small Y–Ti–O nanoclusters with a size ranging between 2 and 5 nm as it is shown in Fig. 3d.

The EBSD maps and histograms of grain misorientation obtained for both types of ODS steel are shown in Figs. 4 and 5. Both histograms exhibit similar trends, but some significant differences can be seen, however. In particular, one can see that a two times higher intensity was measured at low misorientation angles (up to 2°) for the pre-alloyed ODS steel than for the elemental ODS material. In both cases, the intensity falls down then very rapidly up to about 20° and increases again at higher misorientation angles, reaching a maximum intensity at about 45°. It is also noteworthy that the fraction of high-angle grains (>15°) is larger in the case of the elemental ODS steel than in the case of the pre-alloyed ODS steel (Table 3). The ratio of high-angle grain boundaries to low-angle ones is equal to 10.1 in the case of the elemental ODS steel and to 2.3 in the
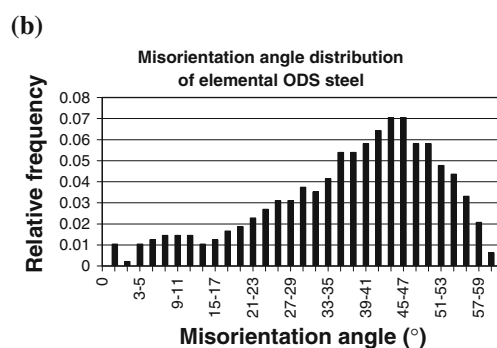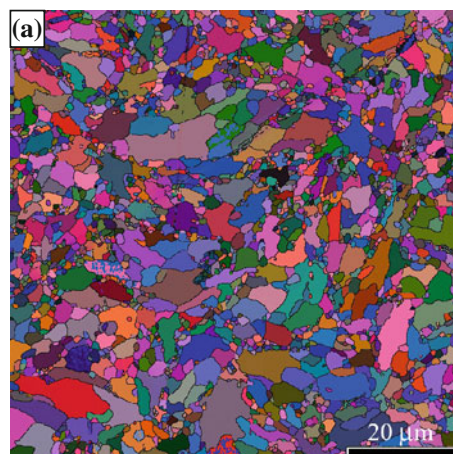

Fig. 4 **a** EBSD map of the elemental ODS steel (Euler angles). The grain boundaries are represented by *black lines*. **b** Histogram of grain angle misorientation
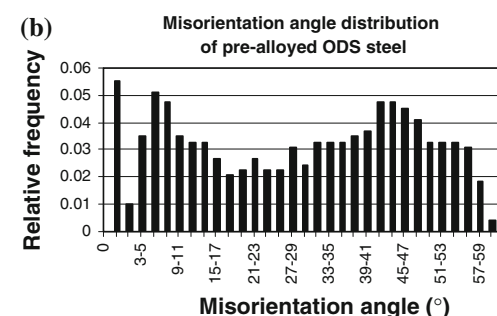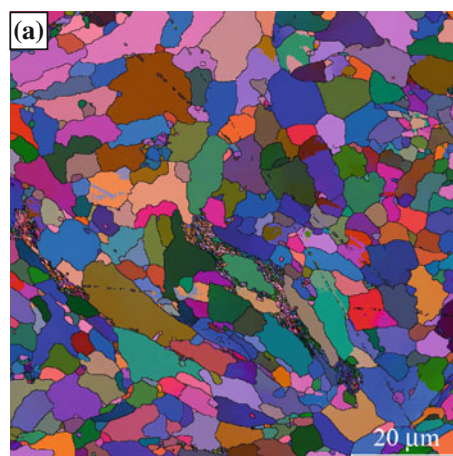

Fig. 5 **a** EBSD map of the pre-alloyed ODS steel (Euler angles). The grain boundaries are represented by *black lines*. **b** Histogram of grain angle misorientation

Table 3 Properties of the ODS ferritic steels after HIPping and heat treatment (HT) at 850 °C for 1 h in vacuum

Ingots	$\mu HV_{0.1}$ As-HIPped	$\mu HV_{0.1}$ HT: 850 °C, 1 h	Density (g/cm^3)	Fraction of high-angle grains (%)
Elemental ODS	368.6 ± 12.7	346.5 ± 5.7	7.778	91.0
Pre-alloyed ODS	428.3 ± 23.4	397.5 ± 14.1	7.801	70.0

case of the pre-alloyed ODS steel. This is because in the pre-alloyed ODS steel a number of coarse grains are actually composed of smaller grains that are slightly misoriented with each other.

These differences in microstructure between the two types of ODS steel are probably due to the different particle sizes in the mechanically alloyed powders and to the different energies accumulated in the powder particles during MA. The dislocations stored in the fine elemental ODS powder can annihilate faster during subsequent high temperature consolidation than the dislocations stored in the coarse pre-alloyed ODS powder, as the dislocations can be faster absorbed by the grain boundaries in the elemental ODS powder (due to a smaller mean free path for dislocations), which results in the formation of high-angle grains. Hence, the microstructure of the elemental ODS steel appears more homogeneous, composed of smaller grains with higher-angle grain boundaries, as compared to the pre-alloyed ODS steel, which might have a significant influence on the respective Charpy impact properties.

Mechanical properties of as-HIPped ingots

Interestingly, hardness tests on as-HIPped materials revealed that the elemental ODS steel exhibits a lower (by about 15%) microhardness of 368 HV$_{0.1}$ than the pre-alloyed one (Table 3). This is probably related to the higher bulk density and dislocation density values measured for the pre-alloyed ODS steel than for the elemental ODS steel (see Fig. 3). The hardness of both materials was slightly reduced (by about 5%) by applying a heat treatment at 850 °C for 1 h. In comparison, the microhardness of the as-HIPped A&D steel prepared from the pre-alloyed powder was 245 HV$_{0.1}$.

The results of Charpy impact tests (absorbed energy vs. testing temperature) are shown in Fig. 6. Both ODS steels exhibit weak Charpy impact properties in comparison to the as-received pre-alloyed steel powder (referred to as A&D) compacted using the same HIPping parameters. Surprisingly, it appears that the elemental ODS steel exhibits better impact properties than the pre-alloyed ODS material, despite its lower density and higher oxygen content. The USE is similar for both ODS steels: 3.1 and 3.2 J for the pre-alloyed and elemental ODS steels, respectively. However, the DBTT of the elemental ODS

steel is almost six times lower (about 25 °C) than the one of the pre-alloyed ODS steel (about 140 °C). It is interesting to note that in the case of the pre-alloyed ODS steel the absorbed energy gradually increases with temperature, which indicates that the ductile-to-brittle transition extends over a wide range of temperatures and which makes difficult to determine precisely the DBTT for this alloy.

SEM images of the fracture surfaces of Charpy impact specimens are shown in Fig. 6. It can be seen that elemental ODS specimens fractured in the LSE region (e.g. −100 °C) exhibit river patterns that are characteristic of a brittle (cleavage) fracture mode (Fig. 6b). Porosity and oxide inclusions can be also seen, which are responsible for initiation of micro-cracks. Both cleavage and ductile fracture modes were observed at testing temperatures corresponding to the DBTT region. Specimens tested at higher temperatures exhibit ductile (dimple) intergranular fracture (Fig. 6c). As known, this type of fracture can occur when precipitates are located at grain boundaries [12]. This confirms that void nucleation, growth and cracking of the specimens at high temperatures occur at the level of the existing precipitates and/or voids.

The unexpected impact fracture properties of the pre-alloyed ODS steel were confirmed by optical microscopy observations of fracture appearance, following Charpy impact tests, as shown in Fig. 7. Such observations showed that the fracture modes of both types of ODS steels are different. At testing temperatures corresponding to the LSE region, from −100 up to 0 °C, the fracture surfaces of all the specimens appear flat and no plastic areas or <10% areas with plastic appearance can be seen, which is typical of a cleavage fracture mode. At 25 °C and above the fracture mode changes from brittle to ductile, and 'cups and cones'-like fracture can be seen for the elemental ODS steel but not for the pre-alloyed ODS steel. Surprisingly, at the higher testing temperature of 200 °C the cleavage fracture mode is still observed in the case of the pre-alloyed ODS steel. At the testing temperature of 300 °C the pre-alloyed ODS steel presents a ductile fracture behaviour that is similar to the one of the elemental ODS steel. Hence, in the case of the pre-alloyed ODS steel the fracture appearance observations seem to indicate that the DBTT of this material is probably higher than the temperature of 140 °C that was obtained by fitting the Charpy impact test results.
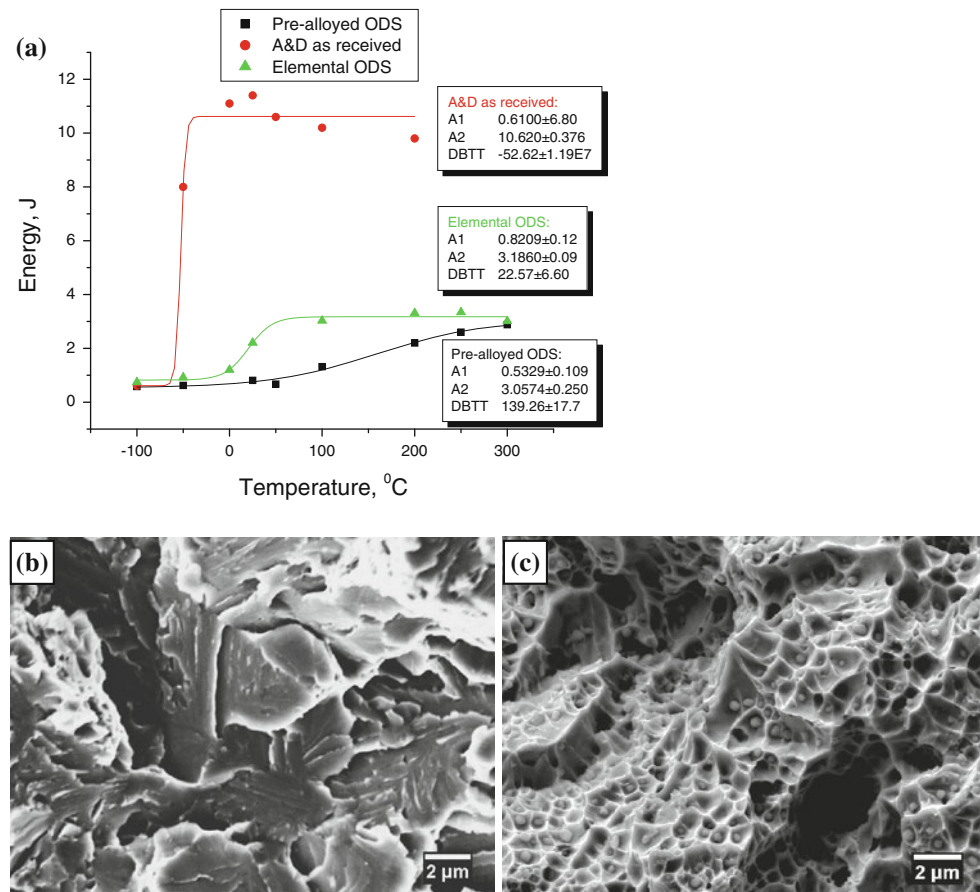
Fig. 6 a Charpy impact properties of the ODS RAF steels after HIPping, and SEM fractographs of the elemental ODS steel tested at **b** −100 °C and **c** 200 °C

Discussion

In this study, the MA of pre-alloyed and elemental powders in two different types of ball mill and using different milling times was performed. Although, in the case of both milling methods, optimization of the process was achieved, which resulted in differences in the milling time, questions about the influence of the ball mill type on the microstructure and mechanical properties of both materials arose. Both ball mills used in this work apply significantly different milling concepts. Planetary ball mill, due to the high centrifugal forces and the high linear velocity of the balls, is considered as high impact energy devices usually used for research purposes due to the small amount of produced powder. Attritors, much larger in size than the planetary ball mills, have a lower impact energy, and milling of the powder is also affected by the shearing force provided by the balls that are driven by a rotating shaft. It is well known that the milling time is related to the energy of the milling device and decreases with increasing impact energy. Suryanarayana reported [13] that the time required to reach a similar particle size in a planetary ball mill and an attritor is

an order of magnitude shorter in the case of the attritor ball mill. This shows that the attritor is a very effective instrument for achieving powder particle size reduction and explains the shorter milling time that was used in the present work. However, in the aim to explicitly determine the influence of both milling methods on Charpy impact properties of as-HIPped ODS steels, the pre-alloyed powder has been mechanically alloyed with 0.3 wt% Y_2O_3 particles in the planetary ball mill for 20 h (i.e. as long as in the attritor). The powder morphology as well as the microstructure and Charpy impact properties of the as-HIPped material are shown in Fig. 8 and summarized in Table 4. Interestingly, it can be seen that the size and shape of these powder particles are similar to the ones of the powder particles mechanically alloyed in the attritor (compare Fig. 1b with Fig. 8a). Moreover, the density, microstructure, microhardness and Charpy impact properties of both pre-alloyed ODS steels are also similar. However, a slightly higher DBTT (by about 10%) has been measured for the pre-alloyed ODS steel prepared using the planetary ball mill, probably due to the higher oxygen amount of 0.188 wt% measured in this material. These
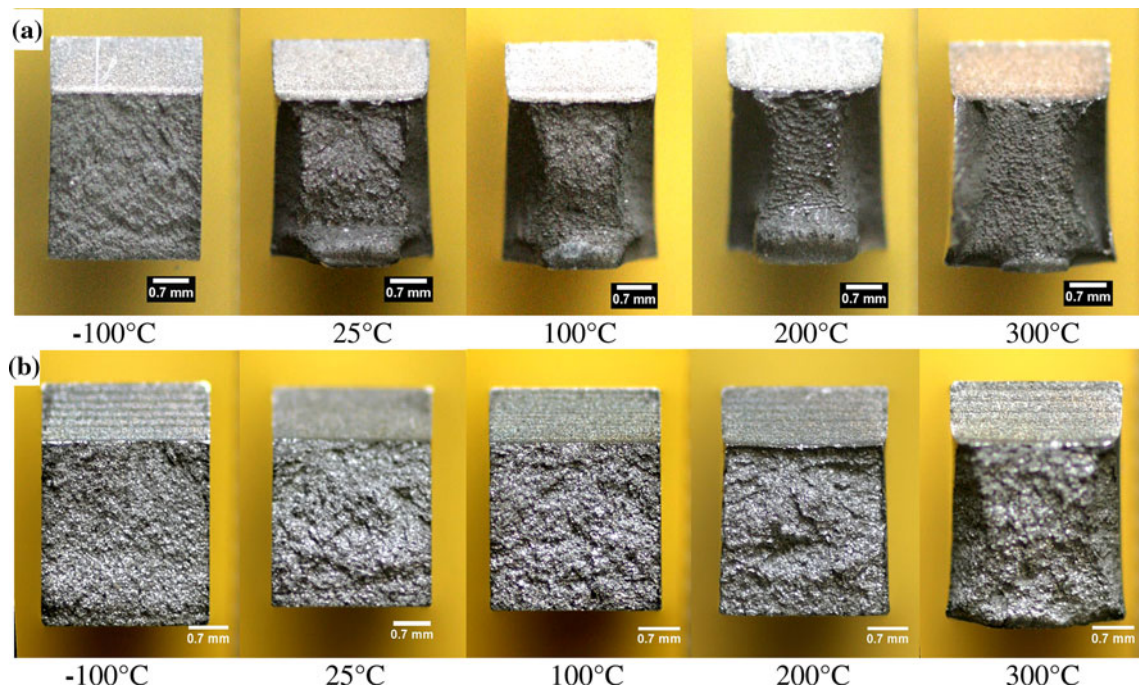
Fig. 7 Optical micrograph of fracture appearance of **a** an elemental ODS steel and **b** a pre-alloyed ODS steel, after HIPping and Charpy impact testing

results confirm that (i) different milling devices (planetary ball mill or attritor) have no significant influence on the Charpy impact properties of as-HIPped pre-alloyed ODS steels and (ii) finer powder particles, in spite of their higher oxygen content, may have a significant and positive influence on the DBTT of as-HIPped ODS steels. Indeed, differences in the elemental and pre-alloyed powder particles are reflected in differences in the microstructure and mechanical performance of both ODS materials. The elemental ODS steel powder particles are finer, more spherical and have a higher surface area than the pre-alloyed ODS steel powder particles that are three times coarser and flat-shaped. Therefore, in spite of the lower oxygen content measured in the pre-alloyed powder and the higher density of the as-HIPped pre-alloyed ODS steel, this material exhibits a more complex microstructure with larger grains (resulting from larger prior powder particles), a higher density of dislocations and a lower volume fraction of high-angle grain boundaries, than the as-HIPped elemental ODS steel, which seems to have a negative influence on the DBTT of the former material.

It is well known from the theory of fracture mechanics, the DBTT of a steel is strongly dependent on (i) the content in impurities (e.g. C, O, N, S and P); the higher the impurity contents the higher the DBTT values, (ii) the grain size: the smaller the grains the lower the DBTT, (iii) the grain misorientation angles: the higher the volume fraction of high-angle grains the lower the DBTT and (iv) the dislocation density: the higher the dislocation density

the higher the DBTT [14]. Indeed, small grains (resulting from fine prior powder particles) with high-angle of misorientation act as effective barriers to crack propagation, which yields a decrease in the DBTT. In addition, it is well known that materials produced from smaller powder particles exhibit a lower DBTT and a larger ductility (i.e. a higher total elongation in tensile tests) than materials produced from larger powder particles, because the contact between powder particles is improved when the particle size is decreased.

It is worth to note that Charpy impact properties of as-HIPped materials are usually lower than those of extruded or wrought materials. This is due to the fact that the HIPping method is very sensitive to the oxygen content in the powder, which may yield the formation of an oxide layer at the surface of the particles, suppress diffusion process during HIPping and cause residual porosity.

The results shown in Fig. 6 also indicate that the USE and DBTT of as-HIPped ODS steels are drastically reduced in comparison to those of the as-HIPped A&D (as-received, no yttria) material. Similar tendencies were also reported in the literature [5, 6, 15]. This problem is not only related to the strengthening effect arising from the presence of yttria nano-particles or to the residual porosity observed after HIPping, but also to the work hardening, solid solution strengthening effect as well as to an increased content in impurities coming from the balls and the jar in the case of ODS steels. An interesting relation between hardness and fracture impact properties was observed by Straffelini
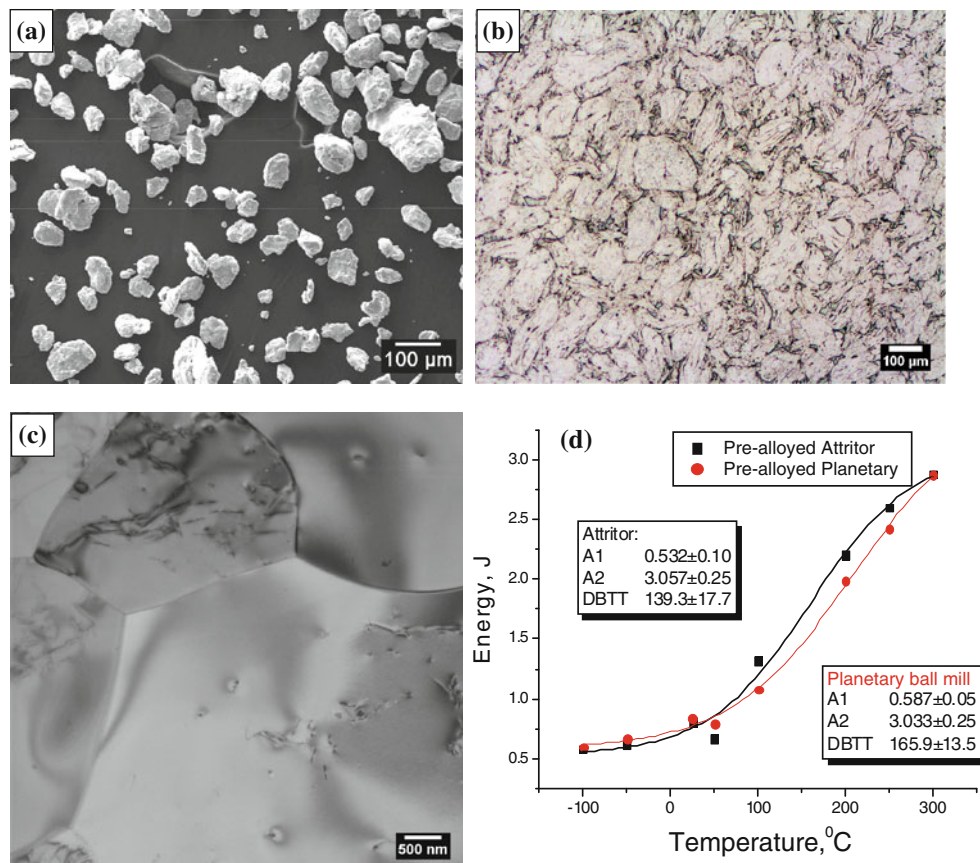
Fig. 8 **a** SEM image of pre-alloyed powder particles after mechanical alloying in a planetary ball mill for 20 h, **b** OM image of the as-HIPped ODS steel, **c** TEM image of the as-HIPped ODS steel and **d** Charpy impact plot of ODS steels prepared using a pre-alloyed powder mechanically alloyed either in an attritor or a planetary ball mill

Table 4 Properties of the ODS ferritic steel after mechanical alloying in a planetary ball mill for 20 h, HIPping and heat treatment (HT) at 850 °C for 1 h in vacuum

ODS steel	$\mu HV_{0.1}$ As-HIPped	$\mu HV_{0.1}$ HT: 850 °C, 1 h	Density (g/cm^3)	DBTT (°C)
Pre-alloyed, mechanically alloyed in a planetary ball mill	426.3 ± 17.0	414.5 ± 24.1	7.80	165.9

et al. [16]. Namely, sintered materials were divided into two groups, those with a lower hardness (below 350 $HV_{0.1}$) and those with a higher hardness (above 350 $HV_{0.1}$). Fracture surface observations of the latter group revealed that, despite of a general ductile fracture mode, the plastic deformation before fracture was noticeably lower in comparison to the former one. Hence, a harder material generally exhibits a more brittle behaviour and weaker Charpy impact properties. The results obtained in this work confirm these observations.

A mechanically alloyed powder may also contain sub-micrometer-sized, closed pores, located inside the powder particles [17]. HIPping of such a kind of powder is very difficult and usually additional thermo-mechanical treatments have to be applied after the first consolidation in order to obtain a fully dense material. A homogenous and fine microstructure, as obtained as the result for such treatments, increases the USE and reduces the DBTT of materials.

Finally, the results of the present studies confirm that the ODS RAF steel produced from elemental powders, despite a higher oxygen content and a lower density, exhibit a lower DBTT value than the ODS RAF steel produced from a pre-alloyed powder, due to a more homogenous, smaller grain size, a higher volume fraction of high-angle grain boundaries and a lower dislocation density in the former material.

Summary

Microstructural observations and Charpy impact tests were performed on Fe–14Cr–2W–0.3Ti–0.3Y$_2$O$_3$ ODS RAF

steels produced either from elemental powders or a pre-alloyed, gas atomized powder using two different ball mills, namely a planetary ball mill and an attritor. After consolidation of the powders it was found that the elemental ODS steel exhibits a much lower DBTT value (about 25 °C) than the pre-alloyed ODS steel (about 140 °C), although the elemental ODS steel powder contains a two times higher oxygen amount than the pre-alloyed ODS steel powder, which affects negatively the density of the elemental ODS steel. However, TEM and SEM–EBSD observations showed that the lower DBTT value measured for the elemental ODS steel results from the smaller grain size, higher volume fraction of high-angle grains and lower dislocation density in this material in comparison to the pre-alloyed ODS steel. Further comparative milling tests of the pre-alloyed, argon-gas atomized powder in a planetary ball mill, under similar conditions and milling time (20 h) as in the case of the attritor, confirmed that the MA device does not seem to have any decisive influence on the DBTT value of as-HIPped ODS steels.

References

1. Chandhok VK, Moll JH (1990) Solid State Phenom 8–9:149
2. Bardos DI (1979) Bimater Med Dev Art Org 7:73
3. Ashworth MA, Bryan JC, Jacobs MH, Davies S (1999) Powder Metall 42(3):243
4. Lind A, Sundstrom J, Peacock A (2005) Fusion Eng Des 75–79:979
5. Ukai S, Fujiwara M (2002) J Nucl Mater 307–311:749
6. Cayron C, Rath E, Ghu I, Launois S (2004) J Nucl Mater 335:83
7. de Castro V, Leguey T, Munoz A, Monge MA, Fernandez P, Lancha AM, Pereja R (2007) J Nucl Mater 367–370:196
8. Ukai S, Mizura A, Yoshitake T, Okuda T, Fujiwara M, Hagi S, Kobayashi T (2000) J Nucl Mater 283–287:702
9. Miller MK, Hoelzer DT, Kenik EA, Russell KF (2004) J Nucl Mater 329–333:338
10. Sakuma D, Yamashita S, Oka K, Ohnuki S, Wakai E (2004) J Nucl Mater 329–333:392
11. Oksiuta Z, Baluc N (2008) J Nucl Mater 374:178
12. Preininger D (2002) J Nucl Mater 307–311:514
13. Suryanarayana C (2001) Progr Mater Sci 46:1
14. Dieter GE (1988) Mechanical metallurgy. McGraw-Hill Book Company, London
15. Gentzbittel JM, Chu I, Burlet H (2002) J Nucl Mater 307–311:540
16. Straffelini G, Menapace C, Molinari A (2002) Powder Metall 45(2):167
17. Chen YL, Jones AR, Miller U (2002) Metall Mater Trans A 33A:2713